NEUROSCIENCE

Adult newborn granule cells confer emotional state–dependent adaptability in memory retrieval

Bo Lei[1,2]†, Bilin Kang[1,2]†, Wantong Lin[3], Haichao Chen[4], Yuejun Hao[1,2], Jian Ma[1], Songhai Shi[1,2,5], Yi Zhong[1,2,5,6]*

Achieving optimal behavior requires animals to flexibly retrieve prior knowledge. Here, we show that adult newborn granule cells (anbGCs) mediate emotional state–dependent adaptability of memory retrieval. We find that acute social reward (aSR) enhances memory retrieval by increasing the reactivation of engram cells, while acute social stress (aSS) weakens retrieval and reduces the reactivation. Such bidirectional regulation relies on the activation of distinct populations of anbGCs by aSR and aSS, triggering opposing modifications of dDG activity, which is sufficient to regulate and predict the performance of memory retrieval. Concordantly, in emotional disorder models, aSR-dependent memory adaptability is impaired, while the effect of aSS remains intact. Together, our data revealed that anbGCs mediate adaptability of memory retrieval, allowing animals to flexibly retrieve memory according to the current emotional state, and suggested the essential roles of anbGCs in translating emotional information to the regulation of memory expression.

INTRODUCTION

Multiple hypotheses suggest that adult hippocampal neurogenesis could provide long-sought mechanisms for linking emotional experiences and memory (1–4). There are two lines of evidence supporting these hypotheses. First, adult hippocampal neurogenesis is profoundly influenced by many behavioral factors (5, 6). Specifically, spatial learning can promote the differentiation of neural progenitor cells and the survival of newborn neurons to increase neurogenesis (7), while voluntary exercise increases the proliferation of neural progenitor cells (8) and environmental enrichment can increase the survival of newborn neurons (9) to promote neurogenesis. Emotional experiences are also reported to be involved in bidirectional regulation of neurogenesis: Chronic stress experiences decline the rate of cell proliferation by increasing the levels of glucocorticoids (10) or inducing neuroinflammation in the hippocampus (11), while social reward can increase neurogenesis via regulating stress-related hormones and optogenetically activating positive memory engram cells in the hippocampus can restore the chronic stress-induced decline of neurogenesis (12). Second, neurogenesis is widely investigated in diverse memory processes via ablating hippocampal neurogenesis or increasing the number of adult newborn granule cells (anbGCs), including pattern separation of contextual memory (13), adaptive forgetting of remote memory (14), and memory flexibility in reversal learning (15). Consistent with these hypotheses, previous studies have revealed that chronic experience-triggered regulation of hippocampal neurogenesis is sufficient to affect memory performance. For instance, voluntary running can lead to adaptive forgetting by increasing hippocampal neurogenesis (14), while chronic stress can cause cognitive functional defects by decreasing hippocampal neurogenesis (11). However, these effects are confined to the change in the number of anbGCs, which takes a long time interval to be effective, and such mechanisms are inadequate to explain the impacts of pervasive daily experiences within a limited time window.

Extensive effort has been devoted to investigating how acute emotional experiences affect the memory process (16, 17), enabling animals to flexibly retrieve memories according to their immediate emotional state. Acute stress can effectively impair memory retrieval in both animal models (18–20) and humans (21, 22), while the novel context, rewarding experiences, and natural emotional stress are capable of enhancing memory acquisition or maintenance (23–25). However, how the hippocampus integrates the impacts of such diverse emotional experiences into distinct modulation of memory performance is still poorly understood.

Here, we have used multiple approaches to examine how daily social experiences modulate memory retrieval and characterize the roles of anbGC activity in mediating such modulation. We found that acute social reward (aSR) and acute social stress (aSS) exert differential impacts on the retrieval but not the formation of contextual fear memory by modifying the reactivation efficacy of engram cells. Such emotional state–dependent bidirectional modulation of memory retrieval is mediated by the activation of distinct populations of anbGCs to trigger opposing regulation of dorsal dentate gyrus (dDG) activity.

RESULTS

Acute social experiences regulate memory retrieval

Although efforts have been devoted to studying the effects of social experience on memory in humans (22, 26), there are few behavioral paradigms available for assaying the impacts of acute daily social experiences on memory in animal models, which strongly limits the further investigation of the related neural mechanisms. Here, we designed two social interaction paradigms to assay the effects of aSR and aSS on memory.

After contextual fear conditioning (CFC), we exposed a conditioned male mouse to two female mice for 10 min as aSR or five grouped male mice as aSS (Fig. 1A and Materials and Methods). When acute social experiences were presented before the retrieval of recent

[1]School of Life Sciences, Tsinghua University, Beijing 100084, P.R. China. [2]McGovern Institute of Brain Research, Beijing 100084, P.R. China. [3]Department of Computer Science, Brandeis University, Waltham, MA 02453, USA. [4]School of Medicine, Tsinghua University, Beijing 100084, P.R. China. [5]Tsinghua-Peking Center for Life Sciences, Tsinghua University, Beijing 100084, P.R. China. [6]MOE Key Laboratory of Protein Sciences, Tsinghua University, Beijing 100084, P.R. China.
*Corresponding author. Email: zhongyithu@tsinghua.edu.cn
†These authors contributed equally to this work.

memory (at 4 or 24 hours after CFC; Fig. 1A), aSR enhanced contextual fear memory retrieval significantly, while aSS reduced it (Fig. 1, B and C). We also used interaction with juvenile mice as aSR and social defeat as aSS, as reported in previous studies (11, 27–30), and observed similar regulatory effects on memory retrieval (fig. S1). However, when acute social experiences were presented immediately before CFC acquisition, both aSR-mediated promotion and aSS-mediated reduction of memory retrieval were abolished (Fig. 1, D to F).

We also tested the locomotion and basal freezing of mice with aSR or aSS and found no impact of aSR or aSS on them (fig. S2, A and B). To further validate the effect of acute social experiences on memory retrieval, we used novel object location test (NOLT) (31) and found that aSR before memory recall significantly promoted memory performance while aSS reduced NOLT memory retrieval (fig. S2, C to E). Thus, our data revealed that acute social experience paradigms could bidirectionally regulate memory retrieval but not the acquisition of
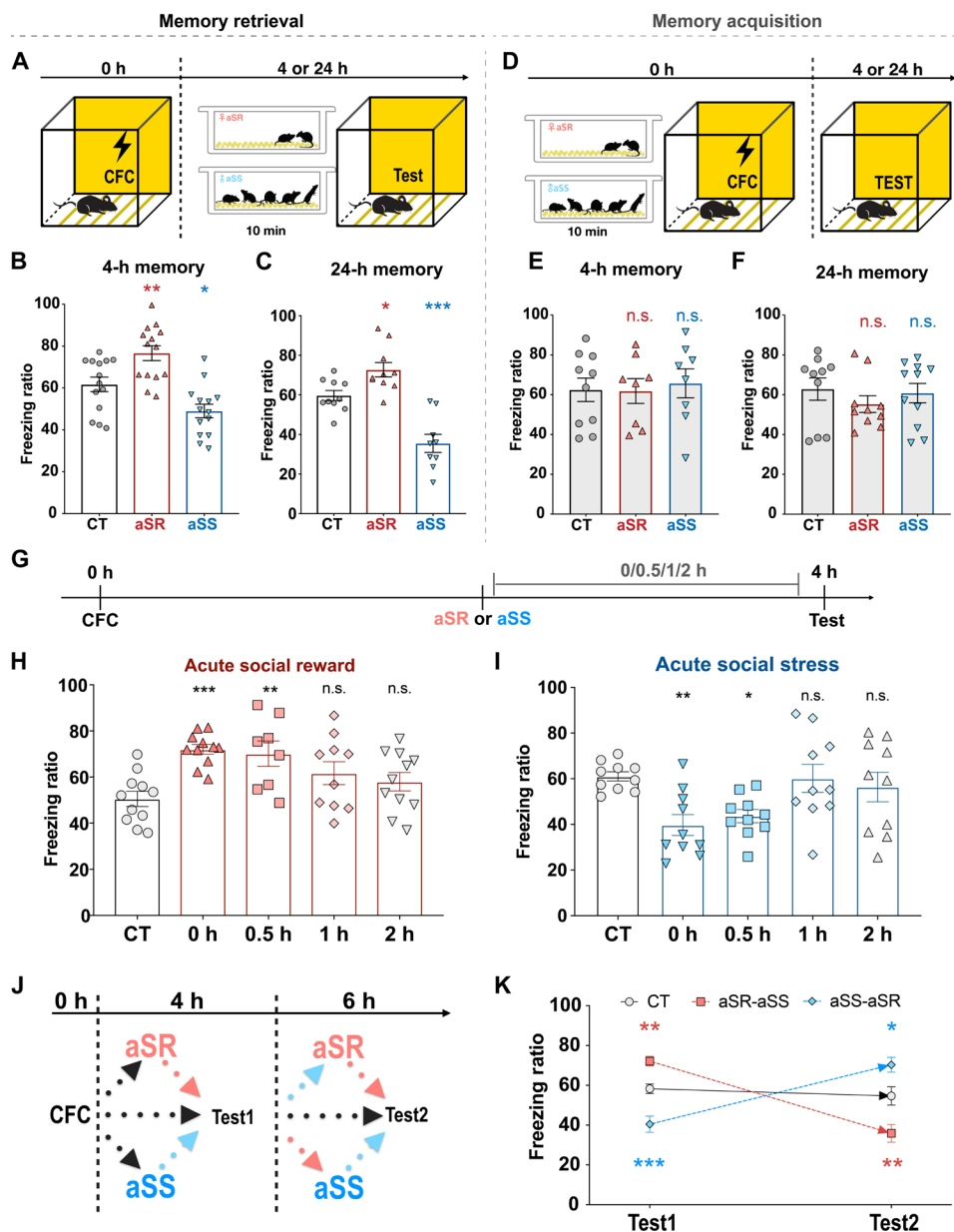

Fig. 1. Acute social experience–dependent bidirectional regulation of retrieving recent contextual fear memory. (**A** and **D**) Experimental schedules of acute social experiences before memory retrieval (A) and memory acquisition (D). (**B** and **C**) Bidirectional regulation of aSR and aSS on retrieval of 4-hour (h) memory [(B), $n_{CT} = 14$, $n_{aSR} = 14$, and $n_{aSS} = 14$] and 24-hour memory [(C), $n_{CT} = 10$, $n_{aSR} = 10$, and $n_{aSS} = 9$]. (**E** and **F**) aSR and aSS before memory acquisition had no effect on 4-hour memory [(E), $n_{CT} = 10$, $n_{aSR} = 8$, and $n_{aSS} = 8$] or 24-hour memory [(F), $n_{CT} = 10$, $n_{aSR} = 10$, and $n_{aSS} = 11$]. (**G**) Experimental schedule of the effective time window of acute social experiences. (**H**) Four-hour memory affected by aSR at different time window ($n_{CT} = 11$, $n_{0h} = 11$, $n_{0.5h} = 8$, $n_{1h} = 10$, and $n_{2h} = 11$). (**I**) Four-hour memory affected by aSS at different time window ($n_{CT} = 10$, $n_{0h} = 10$, $n_{0.5h} = 10$, $n_{1h} = 10$, and $n_{2h} = 10$). (**J**) Experimental schedule of two sequential retrieval tests. (**K**) Reversible regulations of acute social experiences on retrieval ($n_{CT} = 16$, $n_{aSR-aSS} = 16$, and $n_{aSS-aSR} = 16$). *$P < 0.05$, **$P < 0.01$, and ***$P < 0.001$, one-way analysis of variance (ANOVA) with Dunnett's test. Graphs show means ± SEM.

recent memory, which indicate that the efficacy of memory retrieval is adaptive to different emotional states.

We next investigated the dynamics and flexibility of such acute social experience–mediated adaptability of memory retrieval. First, we tested whether this effect is temporary and how long it can maintain. We found that the presentation of acute social experiences was effective only when given immediately or up to 0.5 hours before memory recall and was ineffective if given 1, 1.5, or 2 hours before memory recall (Fig. 1, G to I). Second, we performed two sequential retrieval tests to determine the flexibility of the regulation. The two contextual fear memory tests were 2 hours apart from each other, with every conditioned mouse being subjected to aSR immediately before one test and aSS immediately before another in counterbalanced order (Fig. 1J). Compared to the control group, the mice that experienced aSR immediately before the first test and then experienced aSS immediately before the second test (Fig. 1J) showed enhanced memory performance in the first test and reduced memory performance in the second (Fig. 1K), while the mice that were subjected to aSS and then aSR (Fig. 1J) performed worse in the first test and better in the second (Fig. 1K). Such results indicated that recent contextual fear memory could be strengthened or weakened depending on the acute social experiences that occurred immediately before retrieval. Overall, we observed temporally sensitive, dynamically regulated retrieval depending on acute social experiences.

anbGCs in dDG mediates effects of acute social experiences on memory retrieval

Given that hippocampal neurogenesis is sensitive to diverse experiences (3–10, 12, 32) and shows a profound impact on memory processes (1, 4, 13–15, 33), anbGCs have been suggested to mediate the impacts of experiences on memory performance (1–3). As a test of the possibility that hippocampal neurogenesis is involved in such acute social experience–mediated memory adaptability, we examined whether acute social experience was still effective in mice with declined hippocampal neurogenesis. For this purpose, we irradiated the heads of mice with x-rays, which are thought to be able to significantly block neurogenesis (Fig. 2, A to C) (34, 35), and we found that the effects of acute social experiences on 4-hour memory retrieval were eliminated in the irradiated mice (Fig. 2D). To avoid these results being caused by the side effects of x-ray irradiation, such as induced neuroinflammation within the first month (36), we conducted the behavior experiments 5 weeks after the irradiation treatment. We observed that the x-ray–irradiated mice showed normal basal freezing level (before receiving foot-shock) in the CFC context, normal learning curve during CFC, and normal performance in anxiety-like behavior test (open-field tests; fig. S3, A, E, and I), which was consistent with previous research showing that x-ray irradiation–induced ablation of neurogenesis could not induce depression- or anxiety-like behaviors directly (37). To further confirm the effect of adult neurogenesis ablation, we next applied pharmacological treatment with temozolomide (TMZ) (14), which significantly decreases neurogenesis (fig. S4, A to C) with normal performance of basal freezing, memory acquisition, and anxiety-like behavior (fig. S3, D, H, and L). We observed failed aSR-mediated enhancement and aSS-mediated reduction of memory retrieval in TMZ-treated mice, and such impairment of acute social experience–based memory adaptability was similar to the effects of x-ray irradiation (fig. S4D). We next used retrovirus (RoV)–dependent strategy to specifically label and manipulate anbGCs in the dDG. We injected the RoV to target neural progenitors and their progeny (38, 39) and express the cyclization recombination enzyme (Cre). Then, a Cre-dependent adeno-associated virus (AAV) drove the expression of caspase3 to induce apoptosis in neurons expressing Cre (fig. S4E). Five weeks after the injection of RoV and AAV in the dDG, the number of anbGCs [labeled with doublecortin (DCX)] was significantly reduced in the dDG (fig. S4, F and G), without affecting the number of anbGCs in the ventral DG (fig. S4, I to K) and the performance of basal freezing, memory acquisition, and anxiety-like behavior (fig. S3, B, F, and J). With this manipulation, acute social experiences, whether aSR or aSS, had no influence on 4-hour memory retrieval (fig. S4H).

Furthermore, aged mice (older than 15 months old) with naturally declined neurogenesis (Fig. 3, E and F) (40) and normal performance of basal freezing, memory acquisition and anxiety-like behavior (fig. S3, C, G, and K) also failed to show promoted memory retrieval with aSR and reduced memory retrieval with aSS (Fig. 2G). The data presented confirm the importance of adult hippocampal neurogenesis in mediating the regulation of memory retrieval on the basis of acute social experience.

We next investigate how adult neurogenesis in dDG is involved in such memory adaptability. Previous studies show that the generation and activation of anbGCs can both affect cognitive function, such as memory forgetting (14), cognitive flexibility (1, 15), and pattern separation (13). Since the acute social experience was presented only 10 min before retrieval, we suspected that anbGC activity would play a major role in the regulation of memory retrieval. To test whether anbGCs were activated during acute social experiences, we injected bromodeoxyuridine (BrdU) into mice 6 weeks before CFC to label anbGCs. Then, conditioned mice were perfused 1.5 hours after social interactions to label acute social experience–activated anbGCs by c-Fos and BrdU staining (Fig. 2, H and I) (41, 42). Compared to the control group, both acute social experience groups had increased proportions of c-Fos$^+$ anbGCs in the overall anbGC population (Fig. 2J), confirming the involvement of anbGC activation during acute social experiences.

We next validated the role of such anbGC activation in acute social experience–dependent adaptability of memory retrieval via inhibiting anbGC activity. For this purpose, we crossed two transgenic mouse lines to form a model with inhibitory chemogenetic tool expressed in anbGCs. One transgenic mouse line R26$^{LSL-hM4Di}$ expressed Cre-dependent hM4DGi, the inhibitory designer receptor exclusively activated by designer drugs (DREADD) (43), and the other expressed a tamoxifen (TAM)–inducible Cre^{ERT2} recombinase under the control of the Nestin gene promoter (6). Nes-Cre^{ERT2}; R26$^{LSL-hM4Di}$ double-transgenic mice (referred to as Nes-Gi mice) were injected with TAM to induce hM4DGi expression 5 to 6 weeks before CFC training (Fig. 2K), which limited the expression only in anbGCs at the time we inject the DREADD receptor agonist clozapine-N-oxide (CNO) to make hM4DGi function (Fig. 2L and fig. S6, A and B). The results showed that with inhibiting the anbGCs during social experiences, aSR and aSS both failed to regulate memory retrieval in Nes-Gi mice, while single-transgenic mice showed normal acute social experience–based memory adaptability (Fig. 2M). Thus, the effects of acute social experiences on memory retrieval were mediated by anbGC activity.

We also inhibited anbGC activity specifically during acute social experiences by using optogenetic tool. By using a RoV-based
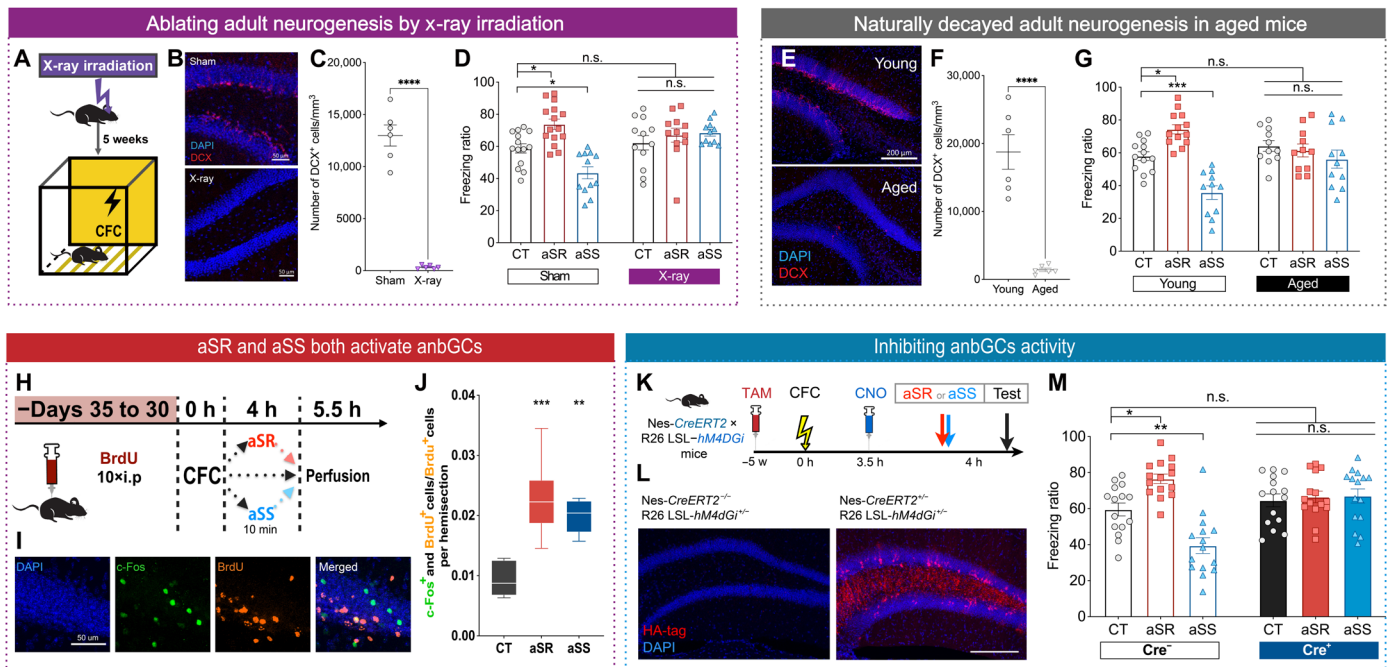
Fig. 2. anbGCs in dDG mediate effects of acute social experiences on memory retrieval. (**A**) Experimental schedule of anbGCs ablation through x-ray irradiation. (**B**) Representative images of anbGCs [labeled by doublecortin (DCX)] in dDG. (**C**) Quantification of anbGCs in the dDG ($n_{Sham} = 6$ and $n_{X-ray} = 6$). (**D**) Four-hour memory in sham group ($n_{CT} = 14$, $n_{aSR} = 15$, and $n_{aSS} = 12$) and x-ray group ($n_{CT} = 12$, $n_{aSR} = 12$, and $n_{aSS} = 11$). (**E**) Representative images of anbGCs (DCX) in the dDG. (**F**) Quantification of anbGCs in the dDG ($n_{Young} = 6$ and $n_{Aged} = 6$). (**G**) Four-hour memory in young mice ($n_{CT} = 13$, $n_{aSR} = 13$, and $n_{aSS} = 11$) and in aged mice ($n_{CT} = 11$, $n_{aSR} = 11$, and $n_{aSS} = 11$). (**H**) Experimental schedule of retrieval-activated anbGC labeling. (**I**) Representative images of retrieval-activated anbGCs (labeled by c-Fos and BrdU). (**J**) Quantification of the ratio of retrieval-activated anbGCs ($n_{CT} = 5$, $n_{aSR} = 6$, and $n_{aSS} = 5$). (**K**) Experimental schedule of inhibiting anbGCs by using double-transgenic mice. (**L**) Representative images of hM4DGi-expressing neurons (labeled by HA tag) in dDG. (**M**) Four-hour memory without anbGC inhibition ($n = 15$ per group) and with anbGC inhibition ($n = 15$ per group). *$P < 0.05$, **$P < 0.01$, ***$P < 0.001$, and ****$P < 0.0001$, unpaired two-tailed t test (C and F), one-way ANOVA with Dunnett's test (J), or two-way ANOVA with Tukey's test (others). Graphs show means ± SEM.

labeling strategy, we expressed optogenetic tool eNpHR3.0 in an-bGCs at a specific age (approximately 4 weeks old; fig. S5, C and D), in conjunction with RoV injected into the dDG at 4 weeks and AAV injected at 2 weeks before CFC (fig. S5, A, B, and G). In the electrophysiological recording of brain slices, optical stimulation reliably silenced RoV-labeled anbGCs expressing eNpHR3.0 (fig. S5, C to F). Inhibiting anbGCs, i.e., stimulating eNpHR3.0 using a 589-nm laser, during acute social experiences blocked the regulatory effect of those experiences on memory retrieval (fig. S4H) without altering social interaction time (fig. S7, E and F), suggesting an essential role of anbGC activation in the acute social experience–dependent regulation of memory retrieval.

anbGCs mediate the effects of aSR and aSS through bidirectional modulation of engram cell reactivation

Since the reactivation of engram cells in the dDG is strongly correlated with memory retrieval performance (*44*–*46*), we assayed engram cell reactivation during memory retrieval with acute social experiences. Engram cells in the dDG were labeled with mCherry during the training sessions by using the c-Fos promoter–driven Tet-off system, as reported in previous studies (*44*, *45*, *47*), and the system was switched off by intraperitoneal doxycycline (Dox) administration 1.5 hours before retrieval (Fig. 3A). To visualize retrieval-activated neurons, we perfused mice 1.5 hours after the recall test for c-Fos staining (Fig. 3, A and B, and fig. S10C). The ratio of

retrieval-reactivated engram cells (mCherry and c-Fos colabeled) to total engram cells (mCherry positive) was significantly increased with aSR and decreased with aSS (Fig. 3C). Thus, aSR-dependent enhancement of memory corresponds to the reactivation of more engram cells upon retrieval, while aSS-dependent decrease of memory corresponds to fewer reactivated engram cells.

To investigate whether the observed modulation of engram cell reactivation depends on anbGCs, we examined the reactivation pattern of engram cells in mice with x-ray irradiation (Fig. 3, D to F). We found that blockade of neurogenesis could abolish both aSR-mediated promotion and aSS-mediated reduction of the engram cell reactivation (Fig. 3G).

aSR and aSS activate distinct anbGC populations

Since the impacts of both aSR and aSS rely on activating anbGCs, the question arises as to how such activation leads to opposing effects. It can be explained by that distinct anbGC populations are recruited via different social experiences. One hypothesis is that memory-related anbGCs are recruited by aSR, while aSS activates others. To test it, we inhibited anbGCs in Nes-Gi mice during training so that they were excluded from encoding memory (Fig. 4A). With such manipulation, we found that aSR failed to regulate memory retrieval (Fig. 4, B and C), while aSS remained effective (Fig. 4, B and C). This result indicates that aSR acts through memory engram anbGCs, while aSS activates non-engram anbGCs.
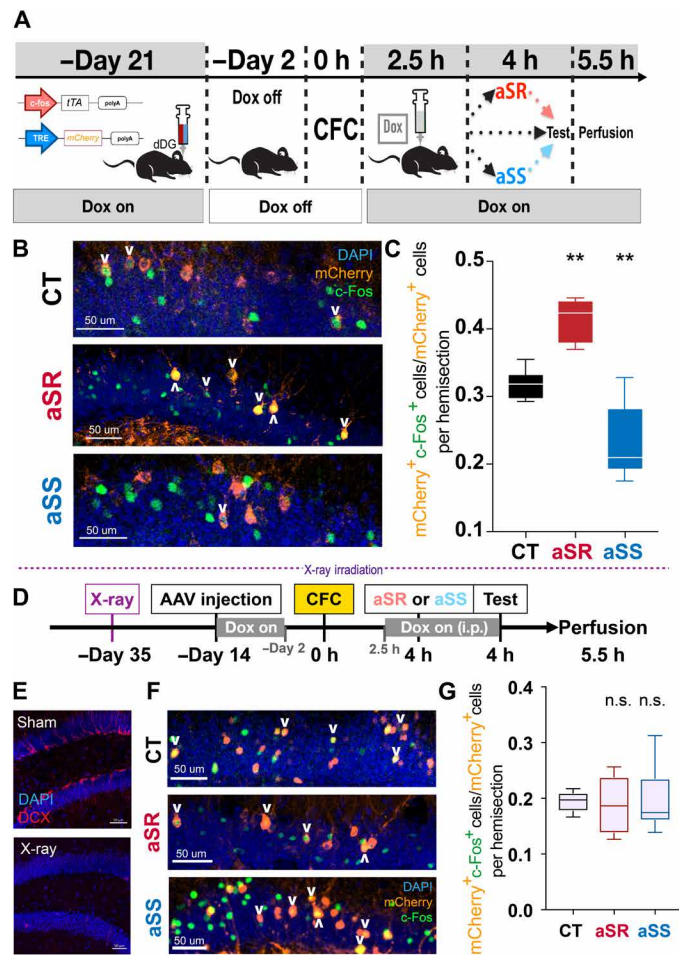
Fig. 3. Acute social experiences modulate engram cell reactivation through anbGCs. (**A**) Experimental design for testing engram reactivation with acute social experiences. (**B**) Representative images of engram cells (mCherry labeled) and retrieval-activated cells (c-Fos labeled) in the dDG. (**C**) Quantification of the engram reactivation ratio ($n_{CT} = 6$, $n_{aSR} = 6$, and $n_{aSS} = 7$). (**D**) Experimental design for testing engram reactivation with acute social experiences in mice with x-ray irradiation. (**E**) Representative images of anbGCs (DCX) in the dDG. (**F**) Representative image of engram cells (mCherry labeled) and retrieval-activated cells (c-Fos labeled) in the dDG. (**G**) Quantification of the engram reactivation ratio in mice with x-ray irradiation ($n_{CT} = 5$, $n_{aSR} = 6$, and $n_{aSS} = 6$). **$P < 0.01$, one-way ANOVA with Dunnett's test. Graphs show means ± SEM.

aSR and aSS trigger opposite modulation of dDG activity

Given that anbGCs played an important role in regulating information processing in the DG by regulating its overall activity (*29, 48, 49*), we hypothesized that aSR and aSS regulate memory by modulating dDG activity in different patterns. We measured dDG activity during acute social experiences by using AAV-expressed GCaMP6f driven by the calcium/calmodulin-dependent protein kinase IIα (CaMKIIα) promoter to record calcium signals in the dDG with an implanted cannula implantation (Fig. 4, D and E). In the first trial, mice were allowed to move freely for 10 min unattended in a new cage with space for rearing. In the second trial, the mice were exposed for 10 min to either two female mice as aSR (Fig. 4F) or five grouped male mice as aSS (Fig. 4I). For aSR, by comparing the ratios ($\triangle F/F$) of calcium signal in the last 200 s of these two trials, we

found that dDG activity was significantly decreased after aSR (Fig. 4, G and H). For aSS, we quantified the calcium signals 60 s before and after the mouse was attacked (the average number of times the tested mouse was attacked during the second trial was 3.25, $n = 8$) and found a sudden increase in dDG activity during each attack (Fig. 4, J and K). In addition, we confirmed that observed GCaMP signal was derived from the change of neuronal activities by recording the enhanced green fluorescent protein (EGFP) signal in dDG during aSS. We found no significant change in EGFP signal after aSS treatment (fig. S9). Consistent with calcium recording, after aSS, the number of c-Fos–positive non-anbGCs (BrdU-negative neurons in dDG granule layer) was significantly increased (fig. S10, A and B).

We then investigated the relationship between this modulation of dDG activity and anbGCs. We found that when neurogenesis was blocked via x-ray irradiation (Fig. 4L), both types of acute social experience failed to trigger changes in calcium activity (Fig. 4, M to P). Collectively, these results showed that aSR and aSS have distinct, anbGC-dependent modulatory effects on dDG activity.

dDG activity is sufficient to regulate and predict memory retrieval

The observed changes in dDG activity likely contribute to the regulation of memory retrieval. To further validate the roles of dDG activity in state-dependent memory adaptability, we altered dDG activity directly through optogenetic manipulation to mimic the regulatory effects of aSR and aSS as a way to confirm the relationship between dDG activity and sequential memory retrieval. Memory performance was significantly enhanced by inhibiting excitatory neuronal activity within the dDG through laser light stimulation of eNpHR3.0, driven by the CaMKIIα promoter, before retrieval (Fig. 5, A to C). Conversely, an increase in dDG activity by stimulation of hChR2 reduced memory retrieval (Fig. 5, E to G). As a control, manipulation of dDG activity did not influence the freezing performance of mice in a novel context (Fig. 5, D and H).

To further investigate the relationship between overall dDG activity and retrieval efficacy, we tested the correlation between dDG neuronal activity before memory recall and retrieval performance. Four hours after training, Ca^{2+} activity in the dDG was recorded for 3 min in freely moving mice in their home cages with the expression of CaMKII-driven GCaMP6f. Immediately after dDG activity recording, mice were tested for memory in the training context (fig. S11A). By combining data from each individual mouse regarding dDG Ca^{2+} activity and memory performance, we found that dDG activity and memory retrieval efficacy had a significant negative correlation (fig. S11, B and C), which was consistent with the results of dDG activity manipulation. Together, our data indicated that dDG activity was sufficient to both regulate and predict the efficacy of memory retrieval. Furthermore, this negative correlation between the efficacy of memory retrieval and overall dDG activity implied that the regulation of activity noise is the neural basis of acute social experience–mediated memory adaptability. We next investigated the relationship between such dDG activity manipulations and acute social experiences. We first inhibited the activity of dDG during aSS and found that such inhibition prevented the aSS-induced decline of memory retrieval (Fig. 5, I and J). We next activated the dDG after aSR and found that the activation also reversed aSR-mediated up-regulation of memory (Fig. 5, K and L). In addition, after optogenetic inhibition, aSS could reverse the effect of dDG inhibition on memory retrieval (fig. S11, D and E), and aSR could prevent the
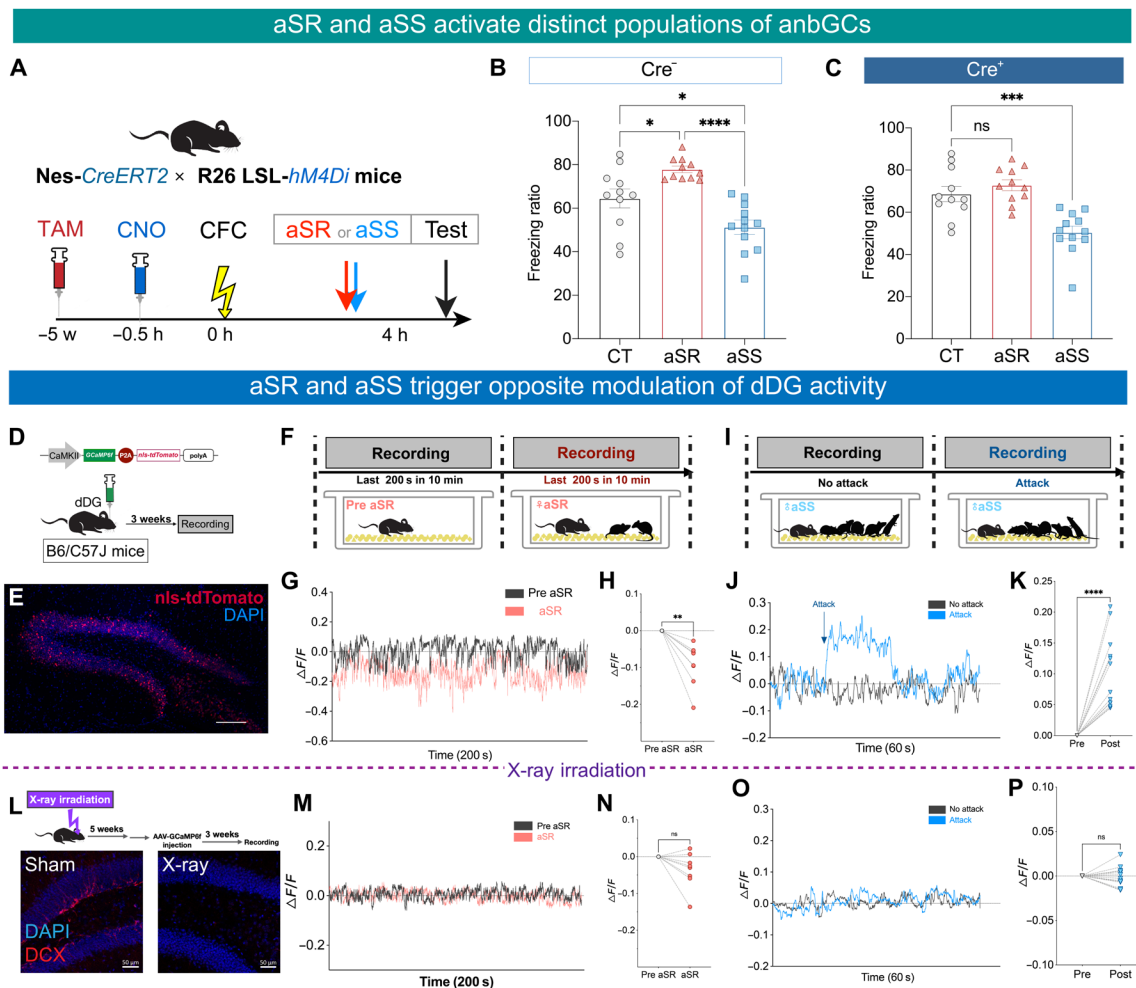
Fig. 4. aSR and aSS activate distinct anbGC populations and trigger opposite modulation of dDG activity. (**A**) Experimental schedule of inhibiting anbGCs during CFC. (**B**) Four-hour memory of Cre⁻ mice ($n_{CT} = 11$, $n_{aSR} = 11$, and $n_{aSS} = 12$). (**C**) Four-hour memory of Cre⁺ mice ($n_{CT} = 11$, $n_{aSR} = 11$, and $n_{aSS} = 12$). (**D**) Experimental schedule of calcium recording. (**E**) Representative image of AAV (mCherry) expression. (**F** and **I**) Experimental schedules of aSR (F) and aSS (I) during calcium recording. (**G** and **J**) Representative diagrams of calcium recording for aSR (G) and aSS (J). (**H**) Comparison of calcium signal between no aSR and aSR ($n = 8$). (**K**) Comparison of calcium signal between pre-attack and post-attack ($n = 7$). (**L**) Experimental schedule of calcium recording in mice with x-ray irradiation (top) and representative images of anbGCs (DCX) in the dDG (bottom). (**M** and **O**) Representative diagrams of calcium recording for aSR (M) and aSS (O) in mice with x-ray irradiation. (**N**) Comparison of calcium signal between no aSR and aSR in mice with x-ray irradiation ($n = 8$). (**P**) Comparison of calcium signal between pre-attack and post-attack in mice with x-ray irradiation ($n = 13$). *$P < 0.05$, **$P < 0.01$, ***$P < 0.001$, and ****$P < 0.0001$, one-way ANOVA with Dunnett's test (B and C) or paired two-tailed t test (others). Graphs show means ± SEM.

decline of memory performance caused by dDG activation (fig. S11, F and G). Together, our data indicate that aSR promotes memory retrieval through inhibiting dDG activity, while aSS elevates dDG activity to decline memory performance.

Consistently, in experiment of detecting engram reactivation (see Fig. 3A), we found that neurons activated by aSS had a higher ratio of non-engram cells (mCherry negative) compared with neurons activated by aSR (fig. S10, C and D), suggesting that aSR enhanced the signal-to-noise ratio of memory by facilitating retrieval-dependent recruitment of engram cells, while aSS reduced the ratio by hindering recruitment and activating more non-engram cells during retrieval. These findings suggest that anbGC-triggered dDG activity modulation reflects the current emotional state and is a key process in the regulation of retrieval efficacy.

Emotional state–dependent memory adaptability is biased in stress models and can be rescued by promoted neurogenesis

Given that depression is a typical emotional disorder and that hippocampal neurogenesis is impaired in many depression models (37, 50), we next tested whether this emotional state–dependent memory adaptability is affected in stress models for the study of depression-related phenotypes. We used two procedures to induce depression-like behaviors in mice, lipopolysaccharide (LPS) injection (Fig. 6A) and chronic forced swimming (CFS; Fig. 6I). For inducing stress model via LPS injection, mice received LPS [intraperitoneally (i.p.)] every day for seven consecutive days (51). For inducing stress model via CFS, mice were individually placed in room temperature water and forced to swim for 10 min each day for 14 consecutive days (52). Both treatments were associated with impairment in the
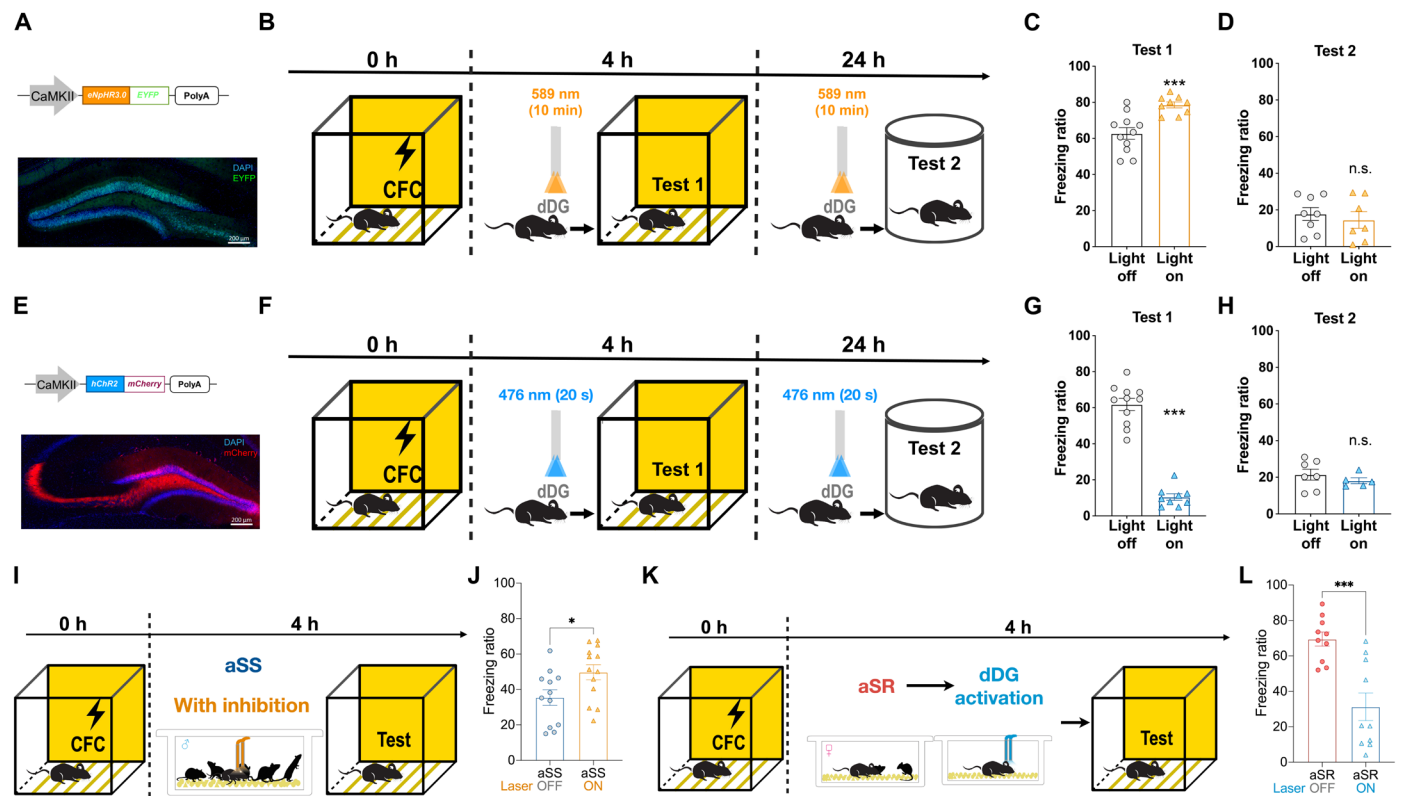
Fig. 5. The sufficiency of dDG activity to regulate memory retrieval performance. (**A** and **B**) Experimental schedule of optogenetic inhibition of dDG neurons before tests. (**C**) Freezing ratio in CFC context with optogenetic inhibition of dDG neurons before test ($n_{Light\ off} = 11$ and $n_{Light\ on} = 9$). (**D**) Freezing ratio in novel context with optogenetic inhibition of dDG neurons before test ($n_{Light\ off} = 8$ and $n_{Light\ on} = 7$). (**E** and **F**) Experimental schedule of optogenetic activation of dDG neurons before tests. (**G**) Freezing ratio in CFC context with optogenetic activation of dDG neurons before test ($n_{Light\ off} = 11$ and $n_{Light\ on} = 9$). (**H**) Freezing ratio in novel context with optogenetic activation of dDG neurons before test ($n_{Light\ off} = 7$ and $n_{Light\ on} = 5$). (**I** and **K**) Experimental schedules. (**J**) Four-hour memory after aSS with dDG inhibition ($n_{OFF} = 12$ and $n_{ON} = 13$). (**L**) Four-hour memory after aSR followed by dDG activation ($n_{OFF} = 10$ and $n_{ON} = 10$). *$P < 0.05$ and ***$P < 0.001$, Pearson's χ^2 test (J) or unpaired two-tailed t test (others). Graphs show means ± SEM.

open-field test (Fig. 6, B and J) and in the tail suspension test (Fig. 6, C and K), which are two parameters for the establishment of depression phenotypes. In these two models, depressed mice showed negatively biased adaptability of memory retrieval; hence, mice did not show enhanced memory retrieval after aSR, while the effect of aSS remained intact (Fig. 6, D and L). In support of this observation, aSR-dependent down-regulation of dDG activity was also blocked (Fig. 6, E, F, M, and N) in both stress models. Furthermore, this biased regulation did not result from alterations in social interaction time during the social reward period (fig. S12). These data are consistent with the biased memory theory in patients with depression (53–55), namely, that those patients have improved negative memory but impaired positive memory.

Given that activating anbGCs or increasing neurogenesis can ameliorate depression-like behaviors in rodents (56–58) and that hippocampal neurogenesis is required for antidepressants to be effective in treating depression (37, 50), we next evaluated whether the promotion of neurogenesis could help mice retain the ability to use positive stimuli to regulate memory retrieval after LPS injection or CFS. We found that 5 weeks of voluntary running could effectively promote neurogenesis (fig. S13). After voluntary running, mice subjected to LPS injection or CFS showed that aSR-dependent

enhancement of memory retrieval remained effective (Fig. 6, G, H, O, and P). To confirm that the effect of voluntary running was caused by increasing neurogenesis, we injected TMZ to specifically block voluntary running–induced neurogenesis (fig. S14, A, D, and E). We found that voluntary running could not rescue the effect of aSR in depressed mice when they were injected with TMZ. Supportively, we used another method to increase neurogenesis via injecting fluoxetine and observed a similar effect with voluntary running (fig. S14, F and G). Our data suggested that in depressed mice, biased acute social experience–based adaptability of retrieval can be ameliorated by increasing neurogenesis.

DISCUSSION
Determining how the hippocampus integrates different emotional information in memory processing is crucial for our understanding of how emotion affects animal behavior. Previous studies have revealed that acute emotional experiences can affect memory through hormone- or catecholamine-triggered modification of synaptic strength (17–20, 23, 25). However, how the hippocampus integrates diverse experiences and how such modification is reflected in specific memory engrams remain elusive. In the current work, we sought to determine how emotional states triggered by acute social experiences affect
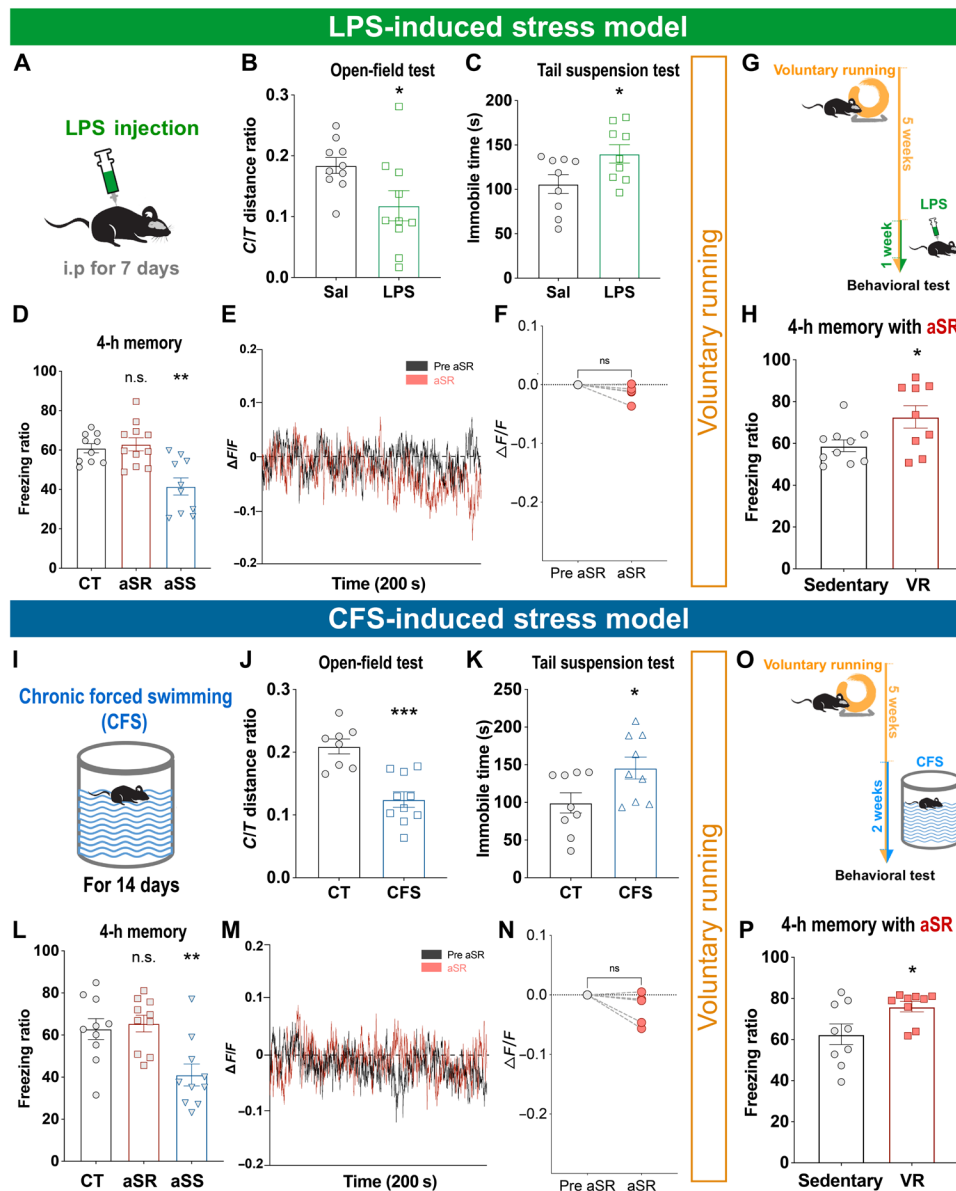
Fig. 6. anbGC-mediated regulation of retrieval is biased in stress models, and the bias can be ameliorated by increasing neurogenesis. (**A**) Stress model induced in mice by LPS injection. (**B**) Open-field tests in LPS-injected mice (n_{Sal} = 10 and n_{LPS} = 10). (**C**) Tail suspension tests in LPS-injected mice (n_{Sal} = 9 and n_{LPS} = 9). (**D**) Four-hour memory with acute social experiences in LPS-injected mice (n_{CT} = 10, n_{aSR} = 11, and n_{aSS} = 10). (**E**) Representative diagram of calcium recording for aSR in LPS-injected mice. (**F**) Comparison of calcium signal between no aSR and aSR in LPS-injected mice (n = 6). (**G**) Experimental schedule of LPS-injected mice with voluntary running (VR). (**H**) Regulation of aSR on 4-hour memory in LPS-injected mice with VR (n_{CT} = 10 and n_{aSR} = 9). (**I**) Stress models induced in mice by CFS. (**J**) Open-field tests in CFS mice (n_{CT} = 8 and n_{CFS} = 10). (**K**) Tail suspension tests in CFS mice (n_{CT} = 9 and n_{CFS} = 9). (**L**) Four-hour memory with acute social experiences in CFS mice (n_{CT} = 10, n_{aSR} = 10, and n_{aSS} = 10). (**M**) Representative diagrams of calcium recording for aSR in CFS mice. (**N**) Comparison of calcium signal between no aSR and aSR in CFS mice (n = 5). (**O**) Experimental schedules of CFS mice with voluntary running (VR). (**P**) Regulation of aSR on 4-hour memory in CFS mice with VR (n_{CT} = 9 and n_{aSR} = 9). *P < 0.05, **P < 0.01, and ***P < 0.001, one-way ANOVA with Dunnett's test (D and L), paired two-tailed t test (F and N), or unpaired two-tailed t test (others). Graphs show means ± SEM.

memory and to identify the neural basis of this emotional state–dependent memory adaptability.

First, we found that retrieval of a hippocampal memory could be up- or down-regulated by acute social events before it within a short time window of 30 min and that aSR led to an enhanced, while aSS led to an attenuated, memory. Such effects were confined to retrieval and did not affect memory acquisition [see Fig. 1 (A to F)]. The pervasive nature of such subtle daily social experiences and

their impact on memory retrieval demonstrate that memory remains plastic even after consolidation. Such adaptability allows the efficacy of memory expression to fluctuate from moment to moment depending on the state immediately before the recall [see Fig. 1 (G to K)], thereby helping animals achieve optimal behavioral outcomes when facing diverse situations.

Second, flexible retrieval of memory is mediated by the activation of two distinct populations of anbGCs: aSR activates training-activated

anbGCs, leading to the recruitment of more engram cells in retrieval, while aSS activates non–training-activated anbGCs, leading to the recruitment of fewer engram cells. The involvement of anbGCs is demonstrated by two observations. First, we observed that aSR and aSS are both capable of activating anbGCs. Second, we found that retrieval adaptability was abolished by the blockade of neurogenesis (see Fig. 2) or optogenetic inhibition of anbGC activity [see Fig. 3 (D to G)]. The involvement of two distinct populations of anbGCs is supported by the following three observations: (i) Excluding anbGCs from engram cells impedes only the effect of aSR and leaves the effect of aSS intact [see Fig. 5 (A to C)]. (ii) aSR and aSS exhibited opposite modulatory effects on dDG neuronal activity, which is mediated by anbGCs, and such modulation is sufficient to regulate and predict performance in memory retrieval (see Figs. 4 and 5). (iii) In stress models, only aSR-induced enhancement in retrieval was impaired, while the aSS effect remains intact, and such impairment could be ameliorated through voluntary running–promoted neurogenesis (see Fig. 6). These three lines of evidence suggest that anbGCs confer adaptability of memory retrieval through two distinct neuronal mechanisms that are activated by positive and negative states. This notion is consistent with recent reports that the activity of anbGCs plays an important role in regulating information processing in the DG through distinct signaling pathways by either activating GABAergic neurons to suppress activity (48) or regulating excitatory synapses via anbGC-activated glutamate receptors (49).

Together, our data demonstrate that the acute emotional state of animals can bidirectionally regulate memory retrieval by activating distinct populations of anbGCs. These data suggest that activation of distinct populations of anbGCs leads to bidirectional modulation of dDG activity that, in turn, affects the reactivation efficacy of engram cells. Such changes in reactivation efficacy determine memory retrieval adaptability. Thus, anbGCs represent a convergence point in the transformation of both positive and negative acute emotional events into appropriate levels of memory retrieval to adapt to an ever-changing environment.

MATERIALS AND METHODS
Animals
All experimental procedures were approved by the Institutional Animal Care and Use Committee of Tsinghua University and were performed using the principles outlined in the Guide for the Care and Use of Laboratory Animals of Tsinghua University. The animal protocol number is 18-ZY1. All C57BL/6J mice were purchased and maintained under standard conditions by the Experimental Animal Center of Tsinghua University. The male mice used throughout the whole study were 8 to 12 weeks old. The female mice used in social reward treatments were 4 to 8 weeks old. The juvenile mice used in social reward treatments were 4 weeks old. The retired male CD-1 breeder mice used in social stress treatments were 6 to 10 months old. Mice containing TAM-inducible Cre recombinase under the control of the Nestin promoter (Nes-Cre/ERT2, stock no. 016261) were purchased from the Jackson Laboratory (Bar Harbor, ME, USA) and were mated to hM4Di floxed mice (R26-LSL-Gi-DREADD, stock no. 026219). Mice were genotyped through polymerase chain reaction using genomic DNA and the Jackson Laboratory–provided primers. TAM induction was performed at 8 weeks of age.

Viral constructs
The AAV$_9$-c-Fos-tTA-pA, AAV$_9$-TRE-mCherry, pAAV-EF1α-DIO-caspase3-P2A-GFP, AAV$_9$-EF1α-DIO-eNpHR3.0-EYFP, AAV$_9$-EF1α-DIO-eNpHR3.0-mCherry, AAV$_9$-EF1α-DIO-mCherry, AAV$_9$-CaMKIIα-eNpHR3.0-EYFP, AAV$_9$-CaMKIIα-hChR2(H134R)-mCherry, and AAV$_9$-CaMkIIα-GCaMP6f-P2A-nls-tdTomato viruses were acquired from Vigene. The pRoV-EF1α-EGFP-2A-Cre and pRoV-EF1α-EGFP viruses were acquired from OBiO. The viral concentration was 1.42×10^{13} viral genomes (vg) ml^{-1} for AAV$_9$-c-Fos-tTA-pA, 1.02×10^{13} vg ml^{-1} for AAV$_9$-TRE-mCherry, 6.59×10^{13} vg ml^{-1} for pAAV-EF1α-DIO-caspase3-P2A-GFP, 2.18×10^{13} vg ml^{-1} for AAV$_9$-EF1α-DIO-eNpHR3.0-EYFP, 5.29×10^{13} vg ml^{-1} for AAV$_9$-EF1α-DIO-eNpHR3.0-mCherry, 1.55×10^{14} vg ml^{-1} for AAV$_9$-EF1α-DIO-mCherry, 1.85×10^{13} vg ml^{-1} for AAV$_9$-CaMKIIα-eNpHR3.0-EYFP, 9.52×10^{13} vg ml^{-1} for AAV$_9$-CaMKIIα-hChR2(H134R)-mCherry, 7.24×10^{13} vg ml^{-1} for AAV$_9$-CaMkIIα-GCaMP6f-P2A-nls-tdTomato, 5.13×10^{7} vg ml^{-1} for pRoV-EF1α-EGFP-2A-Cre, and 1.21×10^{9} vg ml^{-1} for pRoV-EF1α-EGFP. Viruses were subdivided into aliquots and stored at −80°C until use.

Stereotactic injection and optical fiber implant
Mice were anesthetized with 0.5% sodium pentobarbital (70 mg/kg, 350 µl/25 g). Bilateral craniotomies were performed using a 0.5-mm-diameter drill, and 400 nl of the virus was injected into the dDG using a 10-µl NanoFil syringe controlled by UMP3 and Micro4 system (WPI) with a speed of 60 nl/min. The dDG injections were bilaterally targeted to −2.2 mm anteroposterior (AP), ±1.3 mm mediolateral (ML), and −2.0 mm dorsoventral (DV). After the injection, the needle remained in place for 10 min to ensure that the virus spread to the targeted area before it was slowly withdrawn. For mice that need fiber implanting, after withdrawing the needle, a Doric fiber-optic patch cord (core diameter, 200 µm; Doric Lenses) was precisely cut to the optimal length and lowered above the injection site (−2.2 mm AP, ±1.3 mm ML, and −1.8 mm DV). A jewelry screw was screwed into the skull to provide an extra anchor point. Dental cement (Teets Cold Cure; A-M Systems) was applied to secure the optical fiber implant. After surgery, the mice were allowed to recover for at least 2 weeks before all subsequent experiments were performed.

Drugs
Bromodeoxyuridine
BrdU (Sigma-Aldrich) was dissolved in 0.9% saline containing 0.007 mM NaOH and injected (100 mg/kg, i.p.) into mice twice per day at 12-hour intervals for five consecutive days.
Temozolomide
TMZ (Sigma-Aldrich) was dissolved in 0.9% saline containing 10% dimethyl sulfoxide and injected (25 mg/kg, i.p.) per day for four consecutive days. A total of four rounds of treatment (1 week apart) were administered to mice (59).
Clozapine N-oxide
CNO was dissolved in phosphate-buffered saline (PBS) with 0.5% dimethyl sulfoxide and injected into mice expressing hM4DGi (i.p.), 20 min before the behavioral experiments. CNO was administered at 2.5 mg/kg for inhibiting neurons.
Tamoxifen
TAM (Sigma-Aldrich) was dissolved in corn oil at 20 mg/ml and injected (i.p.) at 150 mg/kg for five consecutive days.

Voluntary running

Mice in the voluntary running group were given voluntary access to two running wheels (diameter, 13 cm) placed in their home cages. Mice in the sedentary group were similarly housed but were not given running wheels (8, 14).

X-ray irradiation

Mice were anesthetized with Avertin (250 mg/kg, i.p.) and before being placed under the x-ray irradiation apparatus (Radsource). A lead shield was used to cover the animal's entire body except the head during irradiation. The dose rate was approximately 0.86 gray (Gy)/min at a source-to-skin distance of 13 cm. The irradiation lasted 700 s and delivered a total of 10 Gy (35).

Acute social reward/stress treatment

For the social reward treatment used throughout the whole study, we placed two female mice, aged between 4 and 8 weeks, in a cage (W, 16 cm; D, 28 cm; and H, 13 cm) with soft packing beforehand for 5 to 10 min to acclimate the mice to the new environment. Then, we placed the male mouse to be tested in CFC into the cage for 10 min. For the social stress treatment used throughout the whole study, we placed the male mouse to be tested into a home cage containing five male mice for 10 min. For the social reward treatment using juvenile, we placed two juvenile mice, aged 4 weeks, in the cage (W, 16 cm; D, 28 cm; and H, 13 cm) with soft packing beforehand for 5 to 10 min to acclimate the mice to the new environment. Then, we placed the male mouse to be tested into the cage for 10 min. For social stress induced by social defeat, we placed the male mouse to be tested into a home cage containing a retired male CD-1 breeder mouse (6 to 10 months old) for 10 min.

Behavioral testing

Social interaction test

Mice were subjected to the social reward procedure described above. Experimenters monitored the whole process and recorded the time of intimate interactions between the male mouse and the female mice. Intimate interaction was defined as actions in which the male mice sniffs, chases, or attempts to mate with the female. The experimenters were blinded to the groups during the tests.

Contextual fear conditioning

Fear conditioning was performed on male mice. For fear conditioning, the context was a chamber (W, 18 cm; D, 18 cm; and H, 29 cm) and a grid floor that consisted of 16 stainless steel rods. Subject mice were placed in the conditioning chamber for 2 min before being given five foot shocks (2 s, 0.8 mA, 1 min apart). Four hours after training, mice were placed into the original context and were allowed to explore for 180 s to monitor their freezing behavior. The same procedure was conducted at 24 hours, 48 hours, or 7 days after training, respectively. For Fig. 1 (J and K), we set two sequential retrieval tests at 4 hours after training and 6 hours after training. Four hours after training, the mice's memory performance was first tested for 120 s in the chamber after a 10-min social experience. Two hours later, mice were tested again for 180 s after another 10-min social experience.

Novel object location test

NOLT consisted of a habituation phase, a training phase, and a testing phase. In the first to third days, mice were subject to a chamber (50 cm by 50 cm by 40 cm) with different patterns on the left and right walls without objects. In the fourth day, mice were trained in the chamber with different patterns on the left and right walls. Two same objects were placed near either patterned wall, and mice were allowed to explore the chamber for 10 min. The location of the objects was counterbalanced among each group. Four hours after training, mice were placed into the chamber with the one object placed to a novel location for 5 min. Exploration of object was recorded using an animal behavior video tracking system (ANY-maze) when the animal's nose was pointed at the object with a maximum distance of 2 cm from the object. The heatmap was plotted in the Anymaze software on the basis of the average exploration time of each group of mice.

Open-field test

The open-field test was conducted in an open plastic arena (50 cm by 50 cm by 40 cm). Mice were first placed in the peripheral area with their head toward the wall. Exploration time for 10 min in the peripheral and central areas, respectively, was measured using an automated video-tracking system (ANY-maze software). The central field is defined as a 20 cm–by–20 cm area in the middle of the arena. We used ratio of central distance/total distance to evaluate anxiety-like behavior and used total distance to evaluate locomotion.

Tail suspension test

Mice were suspended by their tails with scotch tape, in a position preventing them from escaping or holding on to nearby surfaces. The immobile time was recorded manually during the 5-min test. The experimenters were blinded to the groups during the tests.

Laser delivery

Inhibition of anbGCs during social experiences

A 589-nm laser was bilaterally delivered by two optic fibers for optogenetical inhibition. Mice to be tested in CFC were first anesthetized by isoflurane for fiber implantation. Then, they experienced either social reward or stress for 10 min. The timing started when the mice recovered from the anesthesia and acted normally. After a 10-min test, mice were anesthetized again to unplug the fiber. After mice recovered from anesthesia for 3 to 5 min, they were tested for memory performance. Control mice were not infected with eNpHR3.0 but were still implanted with the cannula delivering light into the dorsal hippocampus.

Inhibition of dDG activity during social stress

Mice were anesthetized to implant the fiber before light delivery. Light from the 589-nm laser was bilaterally delivered to inhibit dDG activity throughout the 10-min social stress. The timing started when the mice recovered from the anesthesia and acted normally. After social stress, mice were tested for memory performance. The control group was also infected with eNpHR3.0 and implanted with the cannula but without delivering light into the dDG during social stress.

Inhibition of anbGCs during training

Mice were anesthetized before and after light delivery. Light from the 589-nm laser was bilaterally delivered to inhibit anbGCs throughout the training procedure.

Inhibition or activation of dDG neurons

Mice were anesthetized before and after light delivery. Mice were placed into a box that was distinguishable from the training context. Light from a 589-nm laser was bilaterally delivered for inhibition, while hChR2 was stimulated bilaterally at 12 Hz (10-ms pulse width) using a 473-nm laser (10 to 15 mW). hChR2 stimulation was conducted for only 20 to 30 s during the 10-min assessment.

Calcium recording

Calcium signals were measured 3 weeks after viral infection with AAV$_9$-CaMkIIα-*GCaMP6f-P2A-nls-tdTomato* and implantation of a single lateral optical fiber at the dDG. A 40- to 60-s baseline recording of the environment was taken, with the light off, before recording each conditioned mouse. Mice to be recorded were first anesthetized using isoflurane for fiber implantation. When testing the change of dDG activity caused by social interaction, mice were allowed to move freely, unattended, in a non-homecage box for 10 min, and the final 200-s signal was recorded. This procedure was followed by another 10-min recorded exposure of the mouse being recorded to either a pair of female mice (social reward treatment) or five male mice (social stress treatment). Social reward treatment was recorded during the last 200 s of the total 10-min trial, while in the social stress treatment, the no-attack period and the attack periods (before and after the attack) were recorded during the 10-min trial. When testing dDG activity to predict behavior performance, mice were allowed to move freely, unattended, in a non-homecage box, and their calcium signal during the whole 3 min was recorded. When recording mice with expressing EGFP, we put a mouse in a box for 5 min and then put an aggressive CD-1 mouse into the box. After the attack of CD-1 mouse on the tested mouse, we took the CD-1 mouse away to avoid following attack, and the no-attack period and the attack period (before and after the attack) were recorded.

Data of the calcium recording were presented as $\Delta F/F$ versus time (in s). $\Delta F/F$ was computed as $(F(t) - F_0)/F_0$. Fluorescence of GCaMP or EGFP (F) was computed as $(signal_{test} - signal_{basline})/signal_{basline}$. Mean baseline fluorescence was recording in experimental environment for 40 to 60 s preceding each recording. The last 200 s of social reward treatment were compared with the last 200 s of the unattended state. For the social stress treatment, attack periods were compared with no-attack periods.

Electrophysiology and immunohistochemistry for recorded slices

Double-virus system was used to drive the expression of the optogenetic tool eNpHR3.0 that targets age-specific anbGCs in conjunction with pRoV-EF1α-*EGFP-2A-Cre*, injected into the dDG at 4 weeks, and AAV$_9$-EF1α-*DIO-eNpHR3.0-EYFP*, at 2 weeks, before in vitro electrophysiological recording. Brains were removed, and acute cortical slices (300 to 350 μm) were prepared using a vibratome (VT1200S, Leica) in chilled choline solution containing 120 mM choline chloride, 2.6 mM KCl, 26 mM NaHCO$_3$, 1.25 mM NaH$_2$PO$_4$, 7 mM MgSO$_4$, 0.5 mM CaCl$_2$, 1.3 mM ascorbic acid, and 15 mM D-glucose, bubbled with 95% O$_2$ and 5% CO$_2$ on. Slices were kept in artificial cerebral spinal fluid containing 126 mM NaCl, 3 mM KCl, 26 mM NaHCO$_3$, 1.2 mM NaH$_2$PO$_4$, 1.3 mM MgSO$_4$, 2.4 mM CaCl$_2$, and 10 mM D-glucose, bubbled with 95% O$_2$ and 5% CO$_2$, recovered at 32°C for 1 hour and then stored at room temperature before recording. All slice recordings were performed at 34°C. An upright microscope (Olympus) equipped with epifluorescence and infrared differential interference contrast illumination, a charge-coupled device camera, and two water immersion lenses (×10 and ×60) was used to visualize and target recording electrodes to EGFP-expressing neurons located in DG. Short pulses of light (590 nm, 700 mA) were generated by a digital micro-mirror device (Polygon400, Mightex) integrated into the optical path of the microscope through the ×10 objective (fig. S5). PolyScan2 software (Mightex) was used to control the location and shape of the area of stimulation. Microelectrodes (5 to 8 megohms) were filled with an intracellular solution containing 110 mM potassium-gluconate, 20 mM KCl, 2 mM MgCl$_2$, 0.2 mM EGTA, 10 mM Hepes, 4 mM MgATP, 0.4 mM Na$_3$GTP, and 0.3% Neurobiotin (Invitrogen; pH 7.25 and 295 mOsm). Whole-cell recordings were performed with an Axon MultiClamp 700B amplifier and pCLAMP10.6 (Molecular Devices). Series resistance was 10 to 30 megohms and periodically monitored. Data were analyzed using Clampfit.

After recording, slices were incubated in 4% paraformaldehyde (PFA) in PBS at 4°C overnight and then stained with primary antibody chicken anti-GFP (1:1000; Aves, GFP-1010, RRID: AB_2307313) at 4°C for 2 days. Slices were incubated with secondary antibody, including Alexa Fluor 488 donkey anti-chicken (the Jackson Laboratory, 703-545-155, RRID: AB_2340375, 1:500) and Alexa Fluor 546–conjugated streptavidin (Invitrogen) at 4°C overnight. *Z*-series images were acquired using a confocal laser scanning microscope (Olympus FV3000; fig. S5).

Engram labeling

To label the engram cells formed in the dDG during training, we injected a mixture of AAV$_9$-c-Fos-*tTA*-pA and AAV$_9$-TRE-*mCherry* into mice (*47*, *60*). Following virus injection, the mice were fed with diet containing Dox (40 mg/kg). To label the engram cells formed during the CFC, the mice were taken off Dox for 2 days. The mice were then subjected to CFC and injected with Dox (i.p., 5 mg/ml, 10 μl per gram of mouse) 1.5 hours before memory retrieval. When Dox treatment was not stopped in mice, no detectable labeled cells can be seen in the dDG (fig. S8).

Histology
Tissue preparation

A total of 1.5 hours after acute social experiences, retrieval, or training, mice were deeply anesthetized with 2% pentobarbital (160 mg/kg,10 μl/g) and transcardially perfused, first with cold PBS and then with cold 4% PFA. The brains were extracted, postfixed in PFA overnight at 4°C, transferred to a 30% sucrose solution, and then stored at 4°C for 3 days. Next, the brains were coronally sectioned at 60 μm through the DG using a freezing microtome.

Immunohistochemistry

Floating sections were used in all the following immunostaining experiments. Unless otherwise stated, all incubations occurred at room temperature. For c-Fos, DCX, and hemagglutinin (HA)–tag immunostaining, sections were washed three times in 1× PBS and rinsed in 1% Triton X-100 for 15 min before a blocking step in PBS with 0.5% Triton X-100 and 10% normal donkey serum for 1 hour. Incubation with primary antibody was performed at 4°C for 48 hours (rabbit anti-doublecortin: Cell Signaling Technology, 4604; RRID: AB_561007; 1:500; guinea pig anti–c-Fos: Synaptic Systems, 226005; RRID:AB_2800522; 1:500; and rabbit anti–HA-tag: Cell Signaling Technology, 3724, RRID: AB_1549585; 1:1000) in PBS with 0.5% Triton X-100 and 1% normal donkey serum. Sections were then washed three times in PBS and incubated with secondary antibody [donkey anti-rabbit immunoglobulin (IgG) Alexa Fluor 647: 711-605-152, RRID: AB_2492288; donkey anti-GP IgG Cy3: 706-165-148, RRID: AB_2340460, Jackson ImmunoResearch, 1:500] for 2 hours. Sections were then washed three times in PBS and incubated in 4′,6-diamidino-2-phenylindole that was diluted in PBS (1:3000) for 10 min. Next, sections were again washed in PBS three times before being mounted

onto slides and coverslipped with antifade mounting medium (Invitrogen).

For BrdU immunochemistry, slices were washed three times in PBS and then incubated in 2 M HCl for 30 min at 37°C. Next, HCl was removed, slices were washed three times in PBS and then neutralized with 0.1 M sodium borate buffer for 10 min. Sodium borate buffer was removed, and slices were washed three times in PBS. The following steps were identical to those described for the c-Fos/DCX immunostaining, as described above. The sections were stained with primary antibody (rat anti-BrdU: Abcam, ab6326; RRID: AB_305426; 1:500) and secondary antibody (donkey anti-rat IgG Alexa Fluor 647: Jackson ImmunoResearch, 712-605-153; RRID: AB_2340694; 1:500).

Imaging and quantification

Fluorescence was detected using a Zeiss LSM 880 with Airyscan for Figs. 2F and 3E, and an LSM 710 META was used for imaging the other figures with the aid of the ZEN software (black edition). Images were acquired with a ×20 objective, and colocalization was confirmed by a three-dimensional reconstruction of Z-series images.

For cell counting, six unilateral dDG regions across all the sections from one brain sample were chosen randomly. Counting was performed manually using the ZEN software (blue edition). Reported cell counts were calculated by averaging the results from all six sections.

Induction of stress models

CFS-induced stress model

Mice were individually placed in an open cylindrical container (diameter, 20 cm; height, 30 cm), containing room temperature water at depth of 20 cm. Each mouse was forced to swim for 10 min each day for 14 consecutive days. After swimming, mice were dried in a separate box and were then placed back to their home cage (52).

LPS-induced stress model

LPS (Sigma-Aldrich) was dissolved in 0.9% saline and injected (0.5 mg/kg, i.p.) into mice every day for seven consecutive days (51).

Quantification and statistical analysis

The CFC experiments were recorded and analyzed by the software Freeze Frame 3, and the freezing threshold was set uniformly. The open-field tests were recorded and analyzed by the software ANYmaze. The calcium imaging experiments were recorded by the software FiberPhotometry. For the tail suspension tests, the immobile time was recorded manually during the 5-min test, and the experimenters were blinded to the groups during the tests. For the cell counting of imaging works, six unilateral dDG regions across all the sections from one brain sample were chosen randomly. Counting was performed manually using the ZEN software (blue edition). The experimenters were blinded to the groups during the counting.

For calcium imaging experiments, mice that did not show significant response to laser compared to base level were excluded from the data analysis. For other experiments, no data were excluded from the analysis. All behavioral experiments were repeated biologically at least once, and calcium imaging experiments were repeated both technically and biologically at least once.

Statistical tests were performed using GraphPad Prism 7.0. No statistical methods were used to predetermine sample sizes, but our sample sizes are similar to those reported in previous publications. Student's t test was used for the comparison between two groups. One-way analysis of variance (ANOVA) with Dunnett's test was used for comparing a number of groups with a single control group. Two-way ANOVA with Tukey's test was used for comparison of multiple groups with two factors. All tests were two tailed. The sample size and statistical tests used are indicated in the figure legends. The sample size "n" represents the number of mice. A full report of P values and statistics was summarized in the "Statistics information" section in the Supplementary Materials. A P value less than 0.05 was considered statistically significant. The data are shown as means ± SEM [*$P < 0.05$; **$P < 0.01$; ***$P < 0.001$; ****$P < 0.0001$; and nonsignificant (n.s.), $P > 0.05$].

REFERENCES AND NOTES

1. C. Anacker, R. Hen, Adult hippocampal neurogenesis and cognitive flexibility–Linking memory and mood. *Nat. Rev. Neurosci.* **18**, 335–346 (2017).
2. J. B. Aimone, J. Wiles, F. H. Gage, Computational influence of adult neurogenesis on memory encoding. *Neuron* **61**, 187–202 (2009).
3. M. Opendak, E. Gould, Adult neurogenesis: A substrate for experience-dependent change. *Trends Cogn. Sci.* **19**, 151–161 (2015).
4. B. Leuner, E. Gould, Structural plasticity and hippocampal function. *Annu. Rev. Psychol.* **61**, 111–140 (2010).
5. H. Van Praag, G. Kempermann, F. H. Gage, Neural consequences of environmental enrichment. *Nat. Rev. Neurosci.* **1**, 1–8 (2000).
6. A. Dranovsky, A. M. Picchini, T. Moadel, A. C. Sisti, A. Yamada, S. Kimura, E. D. Leonardo, R. Hen, Experience dictates stem cell fate in the adult hippocampus. *Neuron* **70**, 908–923 (2011).
7. P. Ambrogini, R. Cuppini, C. Cuppini, S. Ciaroni, T. Cecchini, P. Ferri, S. Sartini, P. Del Grande, Spatial learning affects immature granule cell survival in adult rat dentate gyrus. *Neurosci. Lett.* **286**, 21–24 (2000).
8. H. van Praag, G. Kempermann, F. H. Gage, Running increases cell proliferation and neurogenesis in the adult mouse dentate gyrus. *Nat. Neurosci.* **2**, 266–270 (1999).
9. G. Kempermann, H. G. Kuhn, F. H. Gage, More hippocampal neurons in adult mice living in an enriched environment. *Nature* **386**, 493–495 (1997).
10. E. Gould, P. Tanapat, Stress and hippocampal neurogenesis. *Biol. Psychiatry* **46**, 1472–1479 (1999).
11. X. D. B. Mckim, A. Niraula, A. J. Tarr, E. S. Wohleb, X. F. Sheridan, J. P. Godbout, Neuroinflammatory dynamics underlie memory impairments after repeated social defeat. 36, 2590–2604 (2016).
12. S. Ramirez, X. Liu, C. J. MacDonald, A. Moffa, J. Zhou, R. L. Redondo, S. Tonegawa, Activating positive memory engrams suppresses depression-like behaviour. *Nature* **522**, 335–339 (2015).
13. T. Nakashiba, J. D. Cushman, K. A. Pelkey, S. Renaudineau, D. L. Buhl, T. J. Mchugh, V. R. Barrera, R. Chittajallu, K. S. Iwamoto, C. J. Mcbain, M. S. Fanselow, S. Tonegawa, Young dentate granule cells mediate pattern separation, whereas old granule cells facilitate pattern completion. *Cell* **149**, 188–201 (2012).
14. K. G. Akers, A. Martinez-Canabal, L. Restivo, A. P. Yiu, A. de Cristofaro, H.-L. L. Hsiang, A. L. Wheeler, A. Guskjolen, Y. Niibori, H. Shoji, K. Ohira, B. A. Richards, T. Miyakawa, S. A. Josselyn, P. W. Frankland, Hippocampal neurogenesis regulates forgetting during adulthood and infancy. *Science* **344**, 598–602 (2014).
15. N. S. Burghardt, E. H. Park, R. Hen, A. A. Fenton, Adult-born hippocampal neurons promote cognitive flexibility in mice. *Hippocampus* **22**, 1795–1808 (2012).
16. M. Joëls, G. Fernandez, B. Roozendaal, Stress and emotional memory: A matter of timing. *Trends Cogn. Sci.* **15**, 280–288 (2011).
17. G. Fernández, R. G. M. Morris, Memory, novelty and prior knowledge. *Trends Neurosci.* **41**, 654–659 (2018).
18. D. J. F. De Quervain, B. Roozendaal, J. L. McGaugh, Stress and glucocorticoids impair retrieval of long-term spatial memory. *Nature* **394**, 787–790 (1998).
19. P. W. Tak, J. G. Howland, J. M. Robillard, Y. Ge, W. Yu, A. K. Titterness, K. Brebner, L. Liu, J. Weinberg, B. R. Christie, A. G. Phillips, T. W. Yu, Hippocampal long-term depression mediates acute stress-induced spatial memory retrieval impairment. *Proc. Natl. Acad. Sci. U.S.A.* **104**, 11471–11476 (2007).
20. J. J. Kim, D. M. Diamond, The stressed hippocampus, synaptic plasticity and lost memories. *Nat. Rev. Neurosci.* **3**, 453–462 (2002).
21. A. M. Smith, V. A. Floerke, A. K. Thomas, Retrieval practice protects memory against acute stress. *Science* **354**, 1046–1049 (2016).

22. S. Kuhlmann, Impaired memory retrieval after psychosocial stress in healthy young men. *J. Neurosci.* **25**, 2977–2982 (2005).

23. T. Takeuchi, A. J. Duszkiewicz, A. Sonneborn, P. A. Spooner, M. Yamasaki, R. G. M. Morris, M. Watanabe, C. C. Smith, G. Fernández, K. Deisseroth, W. Robert, Locus coeruleus and dopaminergic consolidation of everyday memory. *Nature* **537**, 357–362 (2016).

24. A. C. Singer, L. M. Frank, Rewarded outcomes enhance reactivation of experience in the hippocampus. *Neuron* **64**, 910–921 (2009).

25. H. Hu, E. Real, K. Takamiya, M.-G. Kang, J. Ledoux, R. L. Huganir, R. Malinow, Emotion enhances learning via norepinephrine regulation of AMPA-receptor trafficking. *Cell* **131**, 160–173 (2007).

26. T. Takahashi, K. Ikeda, M. Ishikawa, T. Tsukasaki, D. Nakama, S. Tanida, T. Kameda, Social stress-induced cortisol elevation acutely impairs social memory in humans. *Neurosci. Lett.* **363**, 125–130 (2004).

27. R. Nardou, E. M. Lewis, R. Rothhaas, R. Xu, A. Yang, E. Boyden, G. Dölen, Oxytocin-dependent reopening of a social reward learning critical period with MDMA. *Nature* **569**, 116–120 (2019).

28. J. A. Mchenry, J. M. Otis, M. A. Rossi, J. E. Robinson, O. Kosyk, N. W. Miller, Z. A. Mcelligott, E. A. Budygin, D. R. Rubinow, G. D. Stuber, Hormonal gain control of a medial preoptic area social reward circuit. *Nat. Neurosci.* **20**, 449–458 (2017).

29. C. Anacker, V. M. Luna, G. S. Stevens, A. Millette, R. Shores, J. C. Jimenez, B. Chen, Hippocampal neurogenesis confers stress resilience by inhibiting the ventral dentate gyrus. *Nature* **559**, 98–102 (2018).

30. S. A. Golden, H. E. Covington, O. Berton, S. J. Russo, A standardized protocol for repeated social defeat stress in mice. *Nat. Protoc.* **6**, 1183–1191 (2011).

31. M. Leger, A. Quiedeville, V. Bouet, B. Haelewyn, M. Boulouard, P. Schumann-Bard, T. Freret, Object recognition test in mice. *Nat. Protoc.* **8**, 2531–2537 (2013).

32. B. Leuner, E. R. Glasper, E. Gould, Sexual experience promotes adult neurogenesis in the hippocampus despite an initial elevation in stress hormones. *PLOS ONE* **5**, e11597 (2010).

33. Y. Gu, M. Arruda-Carvalho, J. Wang, S. R. Janoschka, S. A. Josselyn, P. W. Frankland, S. Ge, Optical controlling reveals time-dependent roles for adult-born dentate granule cells. *Nat. Neurosci.* **15**, 1700–1706 (2012).

34. M. L. Monje, S. Mizumatsu, J. R. Fike, T. D. Palmer, Irradiation induces neural precursor-cell dysfunction. *Nat. Med.* **8**, 955–962 (2002).

35. T. Kitamura, Y. Saitoh, N. Takashima, A. Murayama, Y. Niibori, H. Ageta, M. Sekiguchi, H. Sugiyama, K. Inokuchi, Adult neurogenesis modulates the hippocampus-dependent period of associative fear memory. *Cell* **139**, 814–827 (2009).

36. N. M. B. Ben Abdallah, L. Slomianka, H.-P. Lipp, Reversible effect of X-irradiation on proliferation, neurogenesis, and cell death in the dentate gyrus of adult mice. *Hippocampus* **17**, 1230–1240 (2007).

37. L. Santarelli, R. Hen, Requirement of hippocampal neurogenesis for the behavioral effects of antidepressants. *Science* **301**, 805–809 (2003).

38. A. Tashiro, C. Zhao, F. H. Gage, Retrovirus-mediated single-cell gene knockout technique in adult newborn neurons in vivo. *Nat. Protoc.* **1**, 3049–3055 (2006).

39. M. S. Fanselow, H. W. Dong, Are the dorsal and ventral hippocampus functionally distinct structures? *Neuron* **65**, 7–19 (2010).

40. H. G. Kuhn, H. Dickinson-Anson, F. H. Gage, Neurogenesis in the dentate gyrus of the adult rat: Age-related decrease of neuronal progenitor proliferation. *J. Neurosci.* **16**, 2027–2033 (1996).

41. M. W. Miller, R. S. Nowakowski, Use of bromodeoxyuridine-immunohistochemistry to examine the proliferation, migration and time of origin of cells in the central nervous system. *Brain Res.* **457**, 44–52 (1988).

42. N. Kee, C. M. Teixeira, A. H. Wang, P. W. Frankland, Preferential incorporation of adult-generated granule cells into spatial memory networks in the dentate gyrus. *Nat. Neurosci.* **10**, 355–362 (2007).

43. B. N. Armbruster, X. Li, M. H. Pausch, S. Herlitze, B. L. Roth, Evolving the lock to fit the key to create a family of G protein-coupled receptors potently activated by an inert ligand. *Proc. Natl. Acad. Sci. U.S.A.* **104**, 5163–5168 (2007).

44. L. G. Reijmers, B. L. Perkins, N. Matsuo, M. Mayford, Localization of a stable neural correlate of associative memory. *Science* **317**, 1230–1233 (2007).

45. T. Kitamura, S. K. Ogawa, D. S. Roy, T. Okuyama, Engrams and circuits crucial for systems consolidation of a memory. *Science* **78**, 73–78 (2017).

46. D. S. Roy, A. Arons, T. I. Mitchell, M. Pignatelli, T. J. Ryan, S. Tonegawa, Memory retrieval by activating engram cells in mouse models of early Alzheimer's disease. *Nature* **531**, 508–512 (2016).

47. X. Liu, S. Ramirez, P. T. Pang, C. B. Puryear, A. Govindarajan, K. Deisseroth, S. Tonegawa, Optogenetic stimulation of a hippocampal engram activates fear memory recall. *Nature* **484**, 381–385 (2012).

48. S. G. Temprana, L. A. Mongiat, S. M. Yang, M. F. Trinchero, D. D. Alvarez, E. Kropff, D. Giacomini, N. Beltramone, G. M. Lanuza, A. F. Schinder, Delayed coupling to feedback inhibition during a critical period for the integration of adult-born granule cells. *Neuron* **85**, 116–130 (2015).

49. V. M. Luna, C. Anacker, N. S. Burghardt, H. Khandaker, V. Andreu, A. Millette, P. Leary, R. Ravenelle, J. C. Jimenez, A. Mastrodonato, C. A. Denny, A. A. Fenton, H. E. Scharfman, R. Hen, Adult-born hippocampal neurons bidirectionally modulate entorhinal inputs into the dentate gyrus. *Science* **364**, 578–583 (2019).

50. B. R. Miller, R. Hen, The current state of the neurogenic theory of depression and anxiety. *Curr. Opin. Neurobiol.* **30**, 51–58 (2015).

51. M. Adzic, J. Djordjevic, M. Mitic, Z. Brkic, I. Lukic, M. Radojcic, The contribution of hypothalamic neuroendocrine, neuroplastic and neuroinflammatory processes to lipopolysaccharide-induced depressive-like behaviour in female and male rats: Involvement of glucocorticoid receptor and C/EBP-β. *Behav. Brain Res.* **291**, 130–139 (2015).

52. R. D. Porsolt, M. le Pichon, M. Jalfre, Depression: A new animal model sensitive to antidepressant treatments. *Nature* **266**, 730–732 (1977).

53. S. G. Disner, C. G. Beevers, E. A. P. Haigh, A. T. Beck, Neural mechanisms of the cognitive model of depression. *Nat. Rev. Neurosci.* **12**, 467–477 (2011).

54. D. G. Dillon, D. A. Pizzagalli, Mechanisms of memory disruption in depression. *Trends Neurosci.* **41**, 137–149 (2018).

55. A. Mathews, C. MacLeod, Cognitive vulnerability to emotional disorders. *Annu. Rev. Clin. Psychol.* **1**, 167–195 (2005).

56. E. Tunc-Ozcan, C.-Y. Peng, Y. Zhu, S. R. Dunlop, A. Contractor, J. A. Kessler, Activating newborn neurons suppresses depression and anxiety-like behaviors. *Nat. Commun.* **10**, 1–9 (2019).

57. A. S. Hill, A. Sahay, R. Hen, Increasing adult hippocampal neurogenesis is sufficient to reduce anxiety and depression-like behaviors. *Neuropsychopharmacology* **40**, 2368–2378 (2015).

58. J. S. Snyder, A. Soumier, M. Brewer, J. Pickel, H. A. Cameron, Adult hippocampal neurogenesis buffers stress responses and depressive behaviour. *Nature* **476**, 458–461 (2011).

59. A. Garthe, J. Behr, G. Kempermann, Adult-generated hippocampal neurons allow the flexible use of spatially precise learning strategies. *PLOS ONE* **4**, e5464 (2009).

60. T. Kitamura, S. K. Ogawa, D. S. Roy, T. Okuyama, M. D. Morrissey, L. M. Smith, R. L. Redondo, S. Tonegawa, Engrams and circuits crucial for systems consolidation of a memory. *Science* **356**, 73–78 (2017).